8(1): 33-44, 2025

Journal of Food and Bioprocess Engineering

Journal homepage: https://jfabe.ut.ac.ir

Original research

# Effect of pulp layer thickness and drying temperature on the drying kinetics and physicochemical quality of tree tomato (*Solanum betaceum*) powder

Isaac M. Maitha [a, *], Michael W. Okoth [a], Lucy G. Njue [a], Duncan O. Mbuge [b]

[a] *Department of Food Science, Nutrition and Technology, University of Nairobi, Kenya*
[b] *Department of Environmental and Biosystems Engineering, University of Nairobi, Kenya*

ABSTRACT

Tree tomato fruits are seasonal and highly nutritious; however, a significant portion of the produce is for immediate consumption owing to their perishability and inadequate preservation methods. To our knowledge, there are no studies that have been conducted on the drying kinetics of tree tomato pulp. Four different pulp layer thicknesses (2, 4, 6, and 8 mm) were dried using a convective oven at air velocities of 15 m/s, set at temperatures of 40, 50, and 60 °C, and then ground into powder. The quality of the powder, drying curves, and the best-fit drying kinetic model to predict the drying behavior were determined. Drying curves across the different temperatures demonstrated that higher temperatures accelerated the drying process for all thicknesses. At 60 °C, materials across all thicknesses showed a rapid reduction in moisture ratio (MR), indicating a faster moisture removal rate. Thicker samples had notably higher MRs across all time points than thinner samples, signifying slower drying rates. The inverse relationship between thickness and drying rate was attributed to increased resistance to moisture diffusion in thicker layers, which slowed the internal water movement to the surface of the materials, decreasing the overall drying rate. Water activity for the dried samples was below 0.6, indicating the product was microbiologically and chemically stable. There was a significant difference for vitamin C, total phenols, and hygroscopicity across the drying temperatures ($p < 0.05$). Samples dried at a temperature of 60 °C recorded higher total phenols, while the hygroscopicity decreased with an increase in temperature. Lower values of vitamin C were recorded at lower drying temperatures.

Keywords: Drying kinetics; Pulp layer thickness; Moisture ratio; Temperature; Tree tomato powder.

Received 29 Jun 2025; Received in revised form 19 Sep 2025; Accepted 17 Oct 2025



## 1. Introduction

Tree tomato (*Solanum betaceum*) is a seasonal crop that produces nutrient-dense, edible, juicy fruits; however, poor postharvest management affects their quality, nutritional, and market characteristics (Maitha et al., 2025). The fruits are climacteric and contain a high amount of water, which makes them susceptible to spoilage and high annual losses. They are also bulky and voluminous, hence causing significant logistical challenges along the value chain. Lack of preparedness for unanticipated emergency times like the Covid-19 pandemic lockdown, when fruit supply is limited and sporadic, requires an alternative for shelf-stable products, as it is difficult to keep sufficient supplies of fresh fruits in the houses (Maitha et al., 2025; García et al., 2016). Sustainable supply of local raw materials remains a challenge to most food industries seeking to improve food quality and safety strategies, which demand novel food products and ingredients like natural food colors (Maitha et al., 2025).

Drying is an essential unit operation after harvesting that uses heat to lower the moisture content of the product by changing the free water into an unavailable form to prevent microbial growth, spoilage, and losses, and ensure safety (Mahanti et al., 2021). It helps reduce handling and transportation costs, increases shelf-stability, and ensures seasonal products are available throughout the year (Verma et al., 2018). It also makes dried products more resistant to chemical reactions and microbial spoilage (Raghavi et al., 2018).

*Corresponding author.
E-mail address: imaitha@uonbi.ac.ke (I. M. Maitha).
https://doi.org/10.22059/JFAB.2025.397640.1204

According to (Inyang et al., 2018), drying is a concurrent heat and mass transfer process, where heat is indirectly or directly supplied to the product, resulting in water evaporation from the product surface and then movement of internal water to the surface of the product (Mahanti et al., 2021). Drying kinetics is an illustration of drying rate against moisture content or drying time that is used to express the process of removing moisture and its connection to the process parameters (Inyang et al., 2018). It is used to predict the drying behavior and optimize the drying variables of different foods (Jideani & Anyasi, 2016). The drying rate is key in food processes for developing the drying kinetic models. Kinetic modeling of process variables helps to describe the changes and their rates quantitatively. It also helps to understand the product's basic reaction mechanisms, essential for safety and quality control modeling (Sharifi et al., 2020). Drying kinetics is important in choosing suitable drying methods, process engineering, and optimization. Hot-air drying methods use equipment like ovens, which are convenient to operate and low in cost (Nadian et al., 2017). However, they affect the product's nutritional and physicochemical quality due to slow heat transfer and long drying time (Chibuzo et al., 2021). The drying process also affects the physicochemical, functional, and technological properties of the end product (Nedamani & Hashemi, 2020). Food products must be handled carefully when drying them because they are quite fragile. Achieving the required quality and final product performance during the drying process depends critically on understanding how the product reacts to heat input.

Tree tomato drying curves are graphs of the moisture versus time, or plots of the rate of water removal versus time. The drying curves help in understanding the "kinetics" of how the tree tomato dries under a specific set of conditions. This concept essentially implies that the changes in the material drying process over time are determined. With the help of drying curves, the drying process can be modified in response to the changes that are occurring. Analyzing data obtained from the drying experiment will provide an understanding of how tree tomato pulp material dries and also assist in determining the best approach to commercial-scale drying of the product.

## 2. Materials and Methods

### *2.1. Raw materials*

About 200 kg of mature, ripe, red tree tomato fruits were procured from five different traders at Marigiti market, Nairobi County, in Kenya. The traders source their tree tomatoes from different regions of Kenya and are the major suppliers in the country. The fruits were transported to the University of Nairobi, Department of Food Science, Nutrition and Technology. They were kept in a cold room at 7 ± 2 °C and 75% relative humidity (Huato- HE174 Data loggers, Shenzhen, China) before further processing.

### *2.2. Study design*

A randomized block experimental design was used to study the effect of temperature and pulp layer thickness on drying kinetics and physicochemical qualities of the tree tomato samples.

### *2.3. Sample preparation*

The fruits were taken from the cold room and blanched in a steam blancher machine set at 120 °C for 3 minutes, after which they were cooled by introducing cold water into the blancher for 3 minutes. The process was followed by pulping using an automatic pulping machine to separate the seeds and peels. It was pasteurized at 60 °C for 5 minutes, then hot-filled immediately into air-tight containers and kept in the cold room at below 7 °C.

### *2.4. Drying experiments*

Drying of the tree tomato pulp samples was done in the Hohenheim HT mini" (Innotech- ingenieursgesellschaft GmbH, Altdorf, Germany) oven cabinet dryer at the Pilot Plant, University of Nairobi. The cabinet dryer is fitted with an air circulation fan, heating power, an automatic exhaust flap for heat regulation, and six perforated trays of 420 x 440 mm each. The dryer was started, and then the temperature was set and attained before each drying experiment was carried out (Mewa et al., 2019).

Six samples of each set of weights were loaded separately onto the trays before the oven was switched on. The air current from the inlet was split and moved between the trays and above the layers of the samples, ensuring even air distribution inside the drying cabinet. The drying was done at a constant airflow (15 m/s) at temperatures of 40, 50, and 60 °C in the oven.

A standard aluminium moisture dish was used as the support on which 2, 4, 6, and 8 mm thick tree tomato pulp was evenly spread, then subjected to the drying process. The pulp layer thicknesses were chosen based on previous trials to maintain consistent spread (Rajoriya et al., 2021).

The sample weights were taken before drying and, as the drying progressed at one-hour intervals, weighed using an electronic precision weighing balance AR3130 KERN® PCB 3500 (Balingen, Germany) and returned to the dryer within a minute's duration. This was repeated until the samples attained constant weight, and then the moisture content for the dried product was calculated. The dried tree tomato samples were then ground into powder using a home blender and aseptically packaged after cooling for further analysis.

### *2.5. Drying kinetics*

Thin-layer mathematical model equations were used to study the drying kinetics of the pulp samples, and the most suitable model was chosen.

#### *2.5.1. Moisture content*

Determination of the initial moisture content of the samples was done according to AOAC test method 967.08 (AOAC, 2010) using Eq. (1).

$$M_t = \frac{(W_o - W) - W_1}{W_1} \quad (1)$$

Where t is time (hours); $M_t$ is the moisture content of the product on a % dry weight basis (DWB); W is evaporated moisture (g); $W_0$ is the sample weight before drying (g); $W_1$ is the sample weight of dry matter (g).

### 2.5.2. Drying rate

The drying rate (DR) of pulp was determined using Eq. (2).

$$DR = \frac{M_t - (M_t + \Delta_t)}{\Delta_t} \quad (2)$$

Where t is time (hours); $M_t$ is moisture content at time; $M_{t+\Delta t}$ is moisture content at time 't+ Δt' on a % dry weight basis (DWB).

The drying curve graphs were presented as DR against moisture content and moisture content against time.

### 2.5.3. Modelling of drying kinetics

The mathematical modeling was done using Fick's second law with moisture ratio (MR) as the dependent variable, as in Eq. (3).

$$MR = \frac{M_t - M_e}{M_o - M_e} \quad (3)$$

Where $M_0$, $M_t$, and $M_e$ represent dimensionless moisture ratio, initial moisture content at time t, and equilibrium moisture content on a % dry weight basis (DWB), respectively.

Since the relative humidity of the sample contact air was not controlled by the drying equipment, and $M_e$ was relatively smaller than $M_t$ and $M_0$, Eq. (3) was shortened to Eq. (4).

$$MR = \frac{M_t}{M_o} \quad (4)$$

The first developed Eq. (5) according to a semi-infinite slab geometry with L thickness and process time frame (t) with i as a positive number (i = 1, 2, 3, …) was therefore simplified to Eq. (6).

$$MR = \sum_{i=0}^{\infty} \frac{8}{(2i+1)^2\pi^2} \cdot \exp\left(\frac{-D_{eff(2i+1)\pi^2 t}}{4L^2}\right) \quad (5)$$

$$MR = \frac{8}{\pi^2} \exp\left(\frac{-D_{eff}\pi^2 t}{4L^2}\right) \quad (6)$$

The effective moisture diffusivity ($D_{eff}$) value, Eq. (7), was obtained by plotting data from lnMR against the drying time.

$$K = \frac{D_{eff}\pi^2}{4L^2} \quad (7)$$

Then the Arrhenius factor was applied in calculating the dependence of $D_{eff}$ as a function of temperature (T), defining activation energy ($E_a$), R as the gas constant (8.314 × $10^{-3}$ kJ/mol), and the Arrhenius factor ($D_0$), as in Eq. (8).

$$D_{eff} = D_0 \exp\left(\frac{E_a}{RT}\right) \quad (8)$$

Experimental moisture values during tree tomato pulp drying were listed as graphs of moisture ratio against drying time and fitted into Logarithmic, Page, Modified Page, Midilli–Kuck, Henderson and Pabis empirical kinetic models, which are commonly used in drying food, as shown in Table 1.

Table 1. Mathematical models fitted to the oven-drying data.

| Model name | Equation | References |
|---|---|---|
| Logarithmic | MR = a exp (−kt) + c | (Inyang et al., 2018) |
| Page | MR = exp ($-kt^n$) | (Inyang et al., 2018) |
| Modified Page | MR = exp ($-(kt)^n$) | (Inyang et al., 2018) |
| Henderson and Pabis | MR = a exp (−kt) | (Inyang et al., 2018) |
| Midilli–Kuck | MR = a exp ($-kt^n$) + bt | (Inyang et al., 2018) |

Where MR is the moisture ratio; a, b, and n are the drying model parameters; k is the drying rate constant (min-1); t is time (min).

Eqs. (9) to (12) were used to calculate goodness of fit, and the most suitable model was chosen for the solar tunnel drying (Loha et al., 2012; Djebli et al., 2020).

$$R^2 = 1 - \frac{\sum_{i=1}^{N}(MR_{cal} - MR)^2}{\sum_{i=1}^{N}(\overline{MR}_{cal} - MR_{exp})^2} \quad (9)$$

$$SSE = \frac{1}{N}\sum_{i=1}^{N}(MR_{exp} - MR_{cal})^2 \quad (10)$$

$$RMSE = \left[\frac{1}{N}\sum_{i=1}^{N}(MR_{cal} - MR_{exp})^2\right]^{\frac{1}{2}} \quad (11)$$

$$X^2 = \frac{\sum_{i=1}^{N}(MR_{cal} - MR_{exp})}{N - Z} \quad (12)$$

Where Z is the number of model parameters; $MR_{exp}$ is experimental MR; N is the number of observations; $MR_{cal}$ is calculated MR.

### 2.6. Quality of tree tomato powder

#### 2.6.1. Physical properties

##### 2.6.1.1. Moisture content

Moisture content (MC) of the fruit powder was determined in triplicate according to (AOAC, 2010) test method 920:151 using Memmert hot air oven (DIN40050-IP20 400, Schwabach, W. Germany) at 105 °C for 3 hours.

##### 2.6.1.2. Water activity (aw)

This was analyzed as described by (Muzaffar & Kumar, 2016). Samples were analyzed in triplicate using a water activity meter (AquaLab TE series 3B Decagon Devices, Inc., Pullman, Washington, USA), which has an accuracy of ± 0.003 at 25 °C and works on the chilled mirror dew point principle to measure the aw of the sample.

##### 2.6.1.3. pH determination

pH of the fruit powder was determined using the procedure described by (Maitha et al., 2025), but with modification. A pH meter (BASIC 20, Crison Instruments, Spain) was used to measure the pH after dissolving 1 gram of the powder sample into 10 mL of distilled water, stirring, and then leaving it to rest for 10 minutes.

##### 2.6.1.4. Color determination

The powder color was determined using a PCE (2014) colorimeter according to the manufacturer's instructions (PCE

Instruments, London, UK). Calibration of the color meter was done against a standard calibration plate of a white surface and set to CIE Standard Illuminant C. The average values of 10 readings were taken as L*, a*, and b*.

The CIE L*a*b* scales were used to evaluate the color, where L* (brightness) 0 = black, and 100 = white; a*(−) = green, and (+) = red; b*(−) = blue, and (+) = yellow.

The measurements were averaged, and total color difference (ΔE) was estimated using Eq. (13).

$$\Delta E = \sqrt{(L_0 * - L_t *)^2 + (a_0 * - a_t *)^2 + (b_0 * - b_t *)^2} \quad (13)$$

Where $L_0 *$, $a_0 *$, and $b_0 *$ are the initial, L∗, a∗, and b∗ values of the samples, while $L_t$, $a_t *$, and $b_t *$ values are the L∗, a∗, and b∗ values at time (t) in days.

### *2.6.1.5. Sensory properties*

The samples were selected, coded, and subjected to sensory analysis as described by (Lawless & Heymann, 2010). Twenty-four panelists from the Faculty of Agriculture, University of Nairobi, were used to assess the sensory attributes of the coded samples on a 7-point hedonic scale (1-dislike extremely, 2-dislike a lot, 3-dislike a little, 4-neither like nor dislike, 5-like a little, 6-like a lot, 7-like extremely). The samples were prepared by weighing 10 grams (one tablespoon full) of powder into clear test cups, coded, and analyzed for color, texture, aroma, and overall acceptability attributes. The aroma was analyzed after reconstituting the sample with drinking water at a ratio of 1:10.

## *2.6.2. Functional properties*

### *2.6.2.1. Antioxidant activity determination*

Hydrophilic antioxidant activity was determined using the 1,1-diphenyl-2-picrylhydrazyl (DPPH) free radical method as described by Maitha et al., 2025.

### *2.6.2.2. Flavonoid content determination*

The aluminum chloride colorimetric method, as described by (Maitha et al., 2025), was used to determine the total flavonoid content. In order to extract the flavonoids, 1 mL of the powder sample was put into a centrifuge tube, topped off with 10 mL of methanol, then vortexed three times for 3 minutes each. A 10 mL flask was filled with approximately 1 mL of the aforementioned methanol extract, topped with 4 mL of distilled water and 0.3 mL of sodium nitrate, and allowed to stand for 5 minutes. The solution was then added to 0.3 mL of 10% aluminum chloride and allowed to settle for 6 minutes. Methanol extract was then mixed with 2 mL of 1 N sodium hydroxide, and the mixture was topped off at 10 mL. The solution was then added to 0.3 mL of 10% aluminum chloride and left for 6 minutes. In addition, 2 mL of 1 N sodium hydroxide was added to the methanol extract. Distilled water was used to top up the solution to 10 mL, and the absorbance was measured at 510 nm with distilled water as the blank. The readings were taken in duplicates, and the concentration of the pulp samples was expressed as mg CE (milligrams of catechin) per 100 g on a dry weight basis.

### *2.6.2.3. Phenolic content determination*

With minor adjustments, the Folin-Ciocalteu technique was utilized to calculate the total phenolic content according to the protocol described by (Snoussi et al., 2021). To remove fat, 0.2 g of dried tree tomato pulp and 2 mL of petroleum ether were placed in a Falcon tube and vortexed for 10 minutes. The sample was allowed to settle, and the supernatant was disposed of. 2 mL each of 80%, 50%, and 70% acetone, all acidified with one milliliter of strong hydrochloric acid, were added to the phenolic extraction mixture, which was then filled to a ten-milliliter capacity with distilled water. After adding 3 mL of the extracted sample mentioned above to 1.5 mL of Folin's reagent, the mixture was centrifuged for 5 minutes, and then 1.2 mL of aq. sodium carbonate solution 7.5% was added. After 30 minutes at room temperature, the sample was measured for absorbance at 765 nm using a Hitachi 2900 UV/VIS spectrophotometer (Tokyo, Japan) with distilled water used as the blank. The concentration of phenolics in the samples was determined using an average calibration curve created from readings for concentrations between 0.25 and 2.0 µg/mL. With readings made in duplicate, the total phenolic component of the tree tomatoes was expressed as milligrams of gallic acid equivalent per gram of extract sample on dry weight basis (mg. GAE.g$^{-1}$DW).

### *2.6.2.4. Vitamin A (Retinol)*

Vitamin A content measurement was carried out as per the method described by (Maitha et al., 2025). About 5 g of the tree tomato powder sample was extracted using 25 cm$^3$ of 95% ethanol for about 20 minutes in a water bath at a temperature range of 60-80 °C. The extract was then cooled and decanted, and the volume (V1) was measured. An 85% ethanol solution was prepared and then chilled for 5 minutes in ice water. A 12.5 cm$^3$ quantity of petroleum ether was added to the cooled ethanol extract, thoroughly mixed to homogenize the sample, and then allowed to stand in a separating funnel to separate into two layers. The bottom layer was separated and returned into the funnel for further extraction using petroleum ether to obtain a fairly yellow extract. All the petroleum ether was collected and returned into the separating funnel for re-extraction using 25 cm$^3$ of ethanol (85%). The transparent layer from the final extract was measured and kept for further analysis. The extract's absorbance was measured using a spectrophotometer (Hitachi 2900 UV/VIS spectrophotometer, Tokyo, Japan) at a wavelength of 436 nm with a blank of petroleum ether. Each sample underwent five rounds of analysis, and average figures were recorded and concentration of Vitamin A (retinol) calculated using Eq. (14).

$$1\ \mu g\ \text{of Vitamin A (retinol)} = 6\ \mu g\ \text{of}\ \alpha - \text{carotene} \quad (14)$$

### *2.6.2.5. Vitamin C determination*

The test was done according to (AOAC, 2010) Official Test Method 967.21-1968 (2010) with slight modification. About 2 mL of the powder sample was titrated with 2,6-dichlorophenolindophenol (DCPIP) solution until the endpoint. The vitamin C content of the tree tomato sample was calculated using Eq. (15) and expressed as mg ascorbic acid per 100 g of sample:

$$\text{Ascorbic acid} = \frac{\text{T.V of DCPIP} \times \text{DCPIP equiv} \times \text{Total volume of extract}}{\text{Volume of sample extract titrated} \times \text{Sample weight}} \times 100 \quad (15)$$

Where T.V is the Titre Value

## *2.6.3. Technological properties*

### *2.6.3.1. Rehydration ratio determination*

Rehydration ratio determination was carried out in a water bath maintained at ambient temperature 25 ± 1 °C as described by (Doymaz, 2014) but with modification. Approximately 1 g of tree tomato powder sample was carefully weighed into a 500 mL beaker,

and 400 mL of distilled water was added, then left to stand for 24 hours. The water was then drained for about 5 minutes, with the excess removed by blotting on tissue paper, before weighing using an electronic precision weighing balance AR3130 KERN® PCB 3500 (Balingen, Germany) and then calculated using Eq. (16).

$$\text{Rehydration Ratio} = \frac{Wm}{Wd}\,(\text{kg}). \quad (16)$$

Where Wm is the weight of moisture (kg), W*d* is the weight of dry matter.

### *2.6.3.2. Hygroscopicity*

Hygroscopicity was analyzed using the method described by (Madani & Sharifi, 2020), with some modifications. 1 g of sample was put in a desiccator having saturated sodium chloride at a relative humidity of 75.29%. Sample weight was checked after a week, and the hygroscopicity results, as adsorbed moisture in grams per 100 grams of dry solids, were calculated using Eq. (17).

$$\text{Hygroscopicity} = \frac{Wf - Wd}{Wd} \times 100. \quad (17)$$

Where Wf and Wd are the weight gained and initial weight, respectively.

### *2.6.3.3. Water solubility index*

The method outlined by (Ordóñez-Santos & Martínez-Girón, 2020), with a few modifications, was used to determine the water solubility index. A suspension of one gram of sample and 100 mL of water was prepared in a beaker, heated in a water bath to 25, 50, and 80 °C, and then stirred at 2500 rpm for 5 minutes. After dispersing the sample, it was centrifuged at 3600 rpm for 5 minutes, then a 25 mL aliquot of the supernatant was transferred into a previously weighed petri dish and dried in an oven at 105 °C until the weight remained constant. Eq. (18) was used to work out the water solubility index (WSI).

$$\text{WSI}(\%) = \frac{Weight\ of\ dissolved\ solid\ in\ supernatant}{Weight\ of\ dry\ solids} \times 100. \quad (18)$$

Where WSI is a water solubility index.

## *2.7. Statistical analysis*

Data obtained from the research was analyzed using R statistics software for Analysis of Variance. R was used to compute the estimates as well as standard errors for various parameters. Drying kinetics and mathematical modelling data analysis were coded in Python for computation, and distribution was done using Anaconda Navigator.

# 3. Results and Discussion

## *3.1. Effect of different pulp layer thicknesses and drying temperatures on the drying kinetics*

The findings of the drying kinetics of tree tomato with varying thicknesses under different drying temperatures were described using moisture ratio as the critical indicator. The analysis involved fitting the drying data to the Modified Page model to quantify drying behavior and observe trends in drying rate constants (k) and the model's exponent parameter (n) for different temperature-thickness combinations. The drying curves at 40, 50, and 60 ºC for the four different pulp layer thicknesses were analyzed and the fitted data was as shown in Figs. 1, 2, and 3.

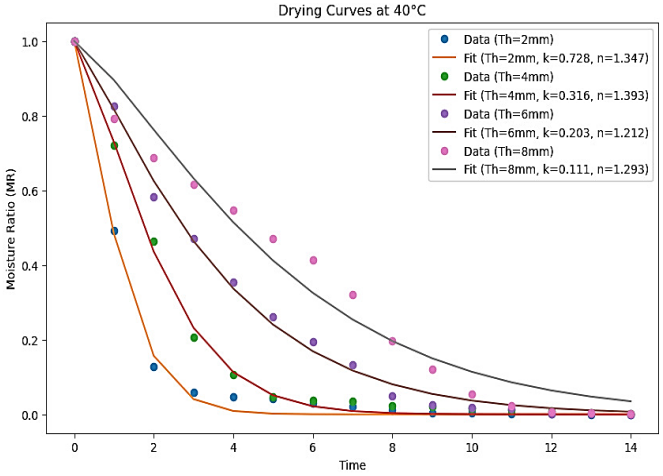


**Fig. 1.** Drying curve of 2, 4, 6, and 8 mm pulp layer thicknesses dried at 40 °C.

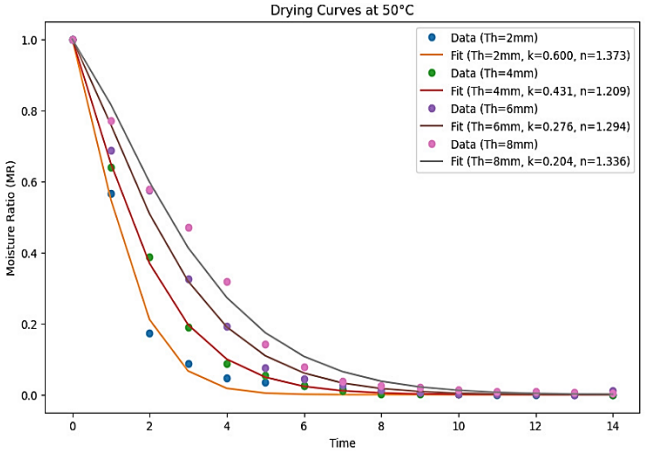


**Fig. 2.** Drying curve of 2, 4, 6, and 8 mm pulp layer thicknesses dried at 50 °C.

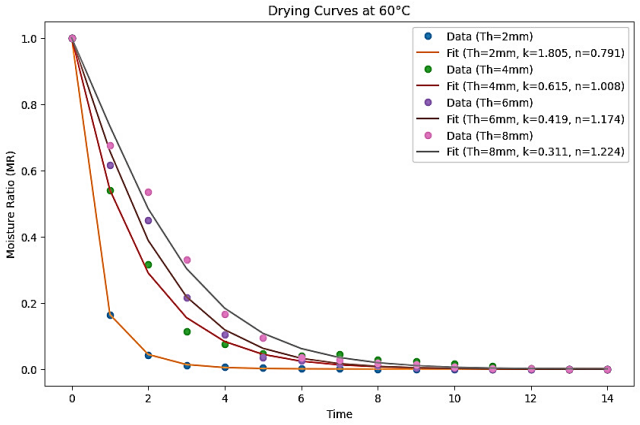


**Fig. 3.** Drying curve of 2, 4, 6, and 8 mm pulp layer thicknesses dried at 60 °C.

The drying curves across the different temperatures (40, 50, and 60 °C) demonstrated that higher temperatures accelerated the drying process for all thicknesses. The graph became gradually flat towards the end of the drying process across all temperatures and thicknesses, signifying that the tree tomato pulp was losing little moisture. During the drying process, the dry matter content of the pulp increased as the water content decreased, and this reduced the rate of moisture removal from the sample. The long drying time at 40 °C could have been caused by the low temperature, which negatively impacted the samples' internal capillary forces, making it difficult for the surface moisture to evaporate fast (Azeez et al., 2019). The decline phase of drying could have been because the internally bound water removal was slow after evaporating all the free surface water (Inyang et al., 2018).

At 60 °C, materials across all thicknesses showed a rapid reduction in MR, indicating a faster moisture removal rate. Higher temperatures also yielded higher drying rate constants (k), which reflect a stronger tendency toward rapid drying. At 60 °C, for instance, even the thickest samples exhibited significantly lower MRs within the same drying duration compared to the lower temperatures.

The effect of thickness on drying rate behavior was prominent, especially at lower temperatures. Thicker samples (6 and 8 mm) had notably higher MRs across all time points than thinner samples (2 and 4 mm), signifying slower drying rates. At 40 °C, the 8 mm sample retained a higher moisture ratio over time compared to the 2 mm sample. The rapid reduction in moisture ratio (MR) signified a fast-drying rate, and the trend aligns with established drying theory, where increased temperatures enhance vapor pressure gradients and kinetic energy of water molecules, expediting diffusion to the material's surface and accelerating moisture loss (Xu et al., 2024).

At the highest drying temperature of 60 °C, the thickest samples had the lowest moisture ratios (MRs), underlining the temperature's role in controlling drying kinetics (Dhande et al., 2024).

This inverse relationship between thickness and drying rate is attributed to increased resistance to moisture diffusion in thicker materials, which slows the internal water movement to the surface, thus decreasing the overall drying rate (Nwakuba et al., 2025).

Fitting the data to the Modified Page model provided valuable insight into the drying process (Bhagya Raj & Dash, 2022). The drying rate constant values (k) increased with temperature for each thickness, and additionally, the thinner materials consistently exhibited higher k values at any given temperature.

Values of n generally remained consistent across all thicknesses at each temperature. The increase in rate constant (k) for each thickness highlighted the positive influence of temperature on drying speed (Kahraman et al., 2021). The consistently higher k values at a given temperature exhibited by the thinner materials supported that reduced thicknesses promote faster moisture diffusion (Van 'T Hag et al., 2020). The constant values of n across all thicknesses suggest that the shape of the drying curve, representing the drying mechanism, is more influenced by temperature than thickness (Liu et al., 2022). This consistency implies a similar moisture removal mechanism across different thicknesses when exposed to the same drying conditions, albeit at different rates (Bhattacharjee et al., 2024).

The MR of a material is usually the proportion of free water that remains uneliminated during the drying process to the total quantity of initially available free water (Dhande et al., 2024). There was a notable difference between the initial and final moisture ratios, due to the initial high moisture content as compared to the low moisture content in the final product after the drying process. The results are in agreement with other studies done that have proved that MR for most agricultural products like mangoes and carrots decreases with an increase in drying time (Akther et al., 2023).

Table 2 shows the effective moisture diffusivities of tree tomato at 40, 50, and 60 °C for 2, 4, 6, and 8 mm. The maximum diffusivities measured were at 60 °C for the 2 mm with a value of 3.325112e-05.

Table 2. Effective moisture diffusivity ($D_{eff}$) for each temperature.

| Temperature (°C) | Thickness (mm) | $D_{eff}$ ($m^2/s$) |
|---|---|---|
| 40.0 | 2 | 2.281023e-05 |
| 40.0 | 4 | 1.116868e-05 |
| 40.0 | 6 | 4.189147e-06 |
| 40.0 | 8 | 3.640550e-07 |
| 50.0 | 2 | 2.533855e-05 |
| 50.0 | 4 | 1.269706e-05 |
| 50.0 | 6 | 4.816127e-06 |
| 50.0 | 8 | 8.969591e-07 |
| 60.0 | 2 | 3.325112e-05 |
| 60.0 | 4 | 1.539380e-05 |
| 60.0 | 6 | 5.052317e-06 |
| 60.0 | 8 | 9.209255e-07 |

The effective moisture diffusivity increased with an increase in temperature, and it quantified the ease with which moisture traversed the tree tomato pulp samples (Van 'T Hag et al., 2020). It denoted the rate at which water in the form of liquid or vapor diffused across a unit area of the pulp samples, which was determined by changes in water vapor pressure and influenced by temperature and the material characteristics (Nwakuba et al., 2025). Higher moisture diffusivity translated to faster moisture flow, which is key during the food drying process, an important unit operation for food preservation that is influenced by the structure of the material, its moisture content, drying temperature, and water bonding interactions (Xu et al., 2024). Moisture diffusivity is a crucial factor in models that forecast material moisture movement, drying kinetics, and performance in industrial processes and a range of engineering.

The activation energy (Ea) increased with an increase in pulp layer thickness (Table 3), with the lowest recorded for the 2 mm pulp layer thickness at 8.0815 KJ/mol.

Table 3. Activation energy for each thickness.

| Thickness (mm) | Activation Energy (KJ/mol) |
|---|---|
| 2 | 8.0815 |
| 4 | 13.939 |
| 6 | 16.414 |
| 8 | 38.666 |

The values were lower compared to the 57.4638 kJ/mol for drying 3 mm thick rhubarb slices (Sharifi et al., 2020). Activation energy, which is the minimal energy required to initiate a chemical reaction, created an activated complex that overcame the pulp layer thickness barrier, which was affecting the drying rate reaction. The increase in pulp layer thickness increased the energy barrier and hence caused an increase in activation energy for the reactants to overcome and result in the dried products (Xu et al., 2024). Decrease in pulp layer thickness augmented the kinetic energy of reactant molecules, hence increasing the probability of activated collisions and subsequent progression of the reaction (Nwakuba et al., 2025).

Table 4. Physical powder properties of 2, 4, 6, and 8 mm pulp layer thicknesses dried at 40, 50, and 60 °C.

| Properties | Drying temp. (°C) | Pulp layer thickness | | | | | |
|---|---|---|---|---|---|---|---|
| | | 2 mm | 4 mm | 6 mm | 8 mm | F-value | P-value |
| **MC** | 40 | 8.994±0.129$^{aA}$ | 8.982±0.017$^{aA}$ | 8.911±0.087$^{aA}$ | 8.962±0.112$^{aA}$ | 0.16 | 0.92 |
| | 50 | 8.584±0.419$^{aA}$ | 8.982±0.017$^{aA}$ | 8.851±0.047$^{aA}$ | 8.862±0.039$^{aA}$ | 0.79 | 0.55 |
| | 60 | 8.294±0.471$^{aA}$ | 8.782±0.217$^{aA}$ | 8.711±0.013$^{aA}$ | 8.577±0.049$^{bA}$ | 0.85 | 0.52 |
| | F-value | 0.89 | 0.84 | 3.14 | 14.43 | | |
| | P-value | 0.49 | 0.51 | 0.18 | 0.005 | | |
| **aw** | 40 | 0.413±0.003$^{aA}$ | 0.408±0.002$^{aA}$ | 0.435±0.015$^{aA}$ | 0.415±0.002$^{aA}$ | 2.79 | 0.15 |
| | 50 | 0.408±0.002$^{aA}$ | 0.408±0.002$^{aA}$ | 0.403±0.003$^{aA}$ | 0.415±0.002$^{aA}$ | 3.84 | 0.091 |
| | 60 | 0.409±0.001$^{aA}$ | 0.408±0.002$^{aA}$ | 0.408±0.002$^{aA}$ | 0.409±0.001$^{aA}$ | 0.37 | 0.78 |
| | F-value | 1.46 | 0.00 | 3.87 | 1.88 | | |
| | P-value | 0.36 | 1.00 | 0.15 | 0.23 | | |
| **pH** | 40 | 3.830±0.010$^{bA}$ | 3.860±0.010$^{aA}$ | 3.845±0.015$^{aA}$ | 3.833±0.008$^{bA}$ | 1.48 | 0.33 |
| | 50 | 3.860±0.010$^{abA}$ | 3.890±0.000$^{aA}$ | 3.885±0.005$^{aA}$ | 3.890±0.012$^{abA}$ | 1.06 | 0.44 |
| | 60 | 3.900±0.010$^{aA}$ | 3.900±0.030$^{aA}$ | 3.910±0.020$^{aA}$ | 3.903±0.016$^{aA}$ | 0.06 | 0.97 |
| | F-value | 12.33 | 1.30 | 4.96 | 7.94 | | |
| | P-value | 0.035 | 0.39 | 0.11 | 0.021 | | |

The same lowercase letters indicate no significant difference across the temperatures, while the same uppercase letters indicate no significant difference among the pulp layer thickness according to the Tukey test at p = 0.05.

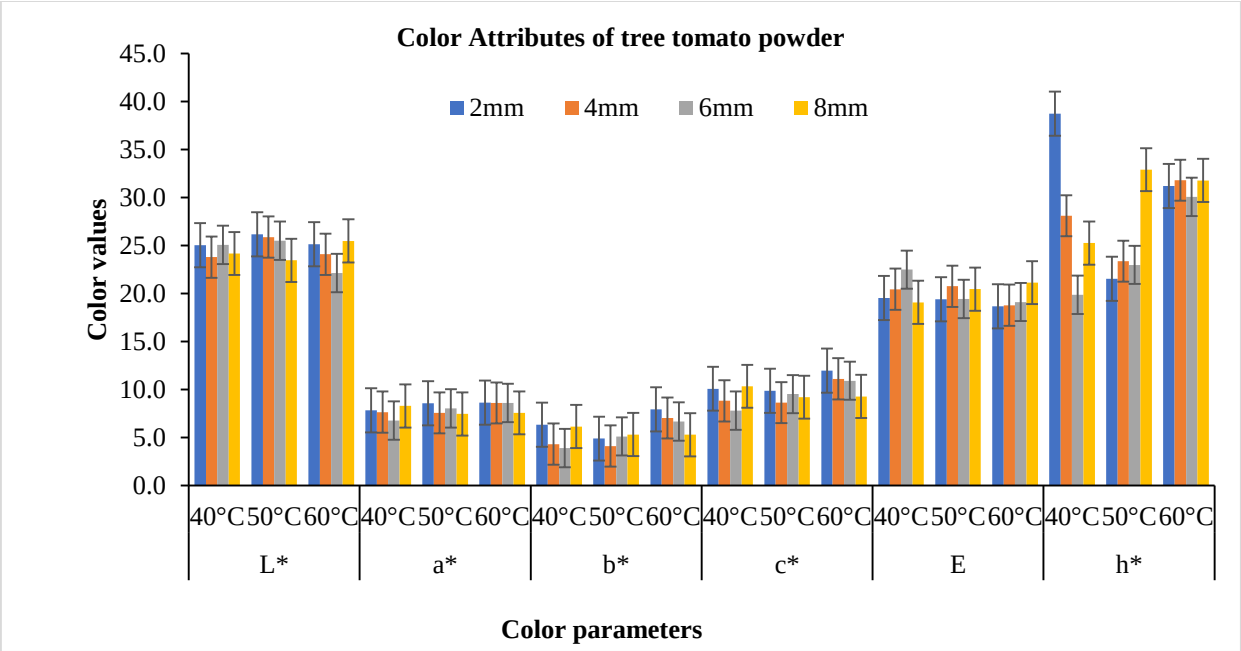


**Fig. 4.** Effect of drying temperatures and pulp layer thickness on the color attributes of tree tomato powder

### *3.2. Effect of pulp layer thickness and drying temperatures on the quality of tree tomato powder*

Table 4 shows the changes in physicochemical properties (moisture content, water activity, and pH values) of tree tomato powder dried at 40, 50, and 60 °C. It is apparent that the moisture content and water activity decreased with an increase in drying temperature, while the pH dropped with a decrease in temperature across all the thicknesses.

The physicochemical properties were affected by the pulp layer thickness and drying temperature. The moisture movement from the samples to the surface, which is usually a result of active diffusion of bound water through the pulp to the drying air, then evaporated and was more exhaustive at higher temperatures and in samples with thinner thicknesses (Rajoriya et al., 2021). The increase in pulp layer thickness also increased the distance and resistance for the movement of water molecules to the surface; hence, some water could have been trapped in the materials, causing the increased moisture content and water activity with increased thickness (Schmidt, 2020). Water activity in the tree tomato powder products, which is the free water available, is responsible for biochemical reactions and microbial activity, which affects the quality of the product (Tapia et al., 2020). The powder product had a water activity below 0.6, indicating it was microbiologically and chemically stable (Dufera et al., 2023). The low pH, which was recorded after an increase in thickness and a decrease in temperature, could have been caused by chemical reactions of the samples and catalyzed by the moisture.

The influence of the drying process on the color parameters is shown in Fig. 4. The pulp layer thickness and temperature significantly ($p < 0.05$) affected the color parameters. There was a

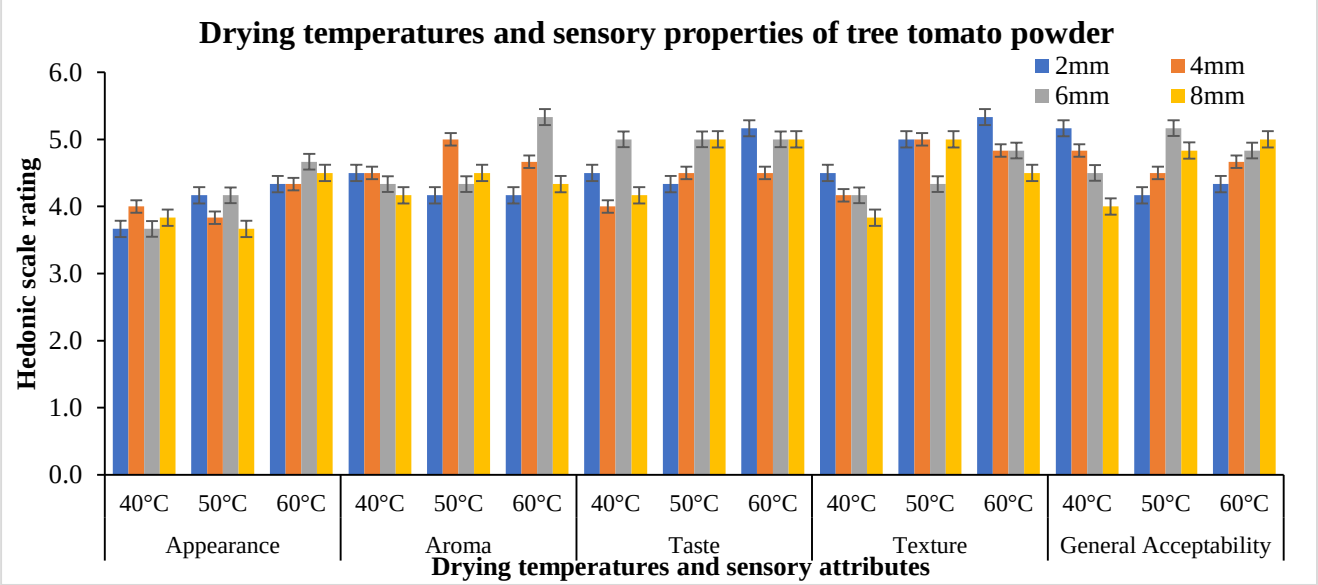


**Fig. 5.** Effect of drying temperatures and pulp layer thickness on the sensory attributes of tree tomato powder

Table 5. Functional powder properties of 2, 4, 6, and 8 mm pulp layer thicknesses dried at 40, 50, and 60 °C.

| Properties | Drying temp. (°C) | Pulp layer thickness | | | | | |
|---|---|---|---|---|---|---|---|
| | | 2 mm | 4 mm | 6 mm | 8 mm | F-value | P-value |
| **Antioxidant activity** | 40 | 1662.46±0.51$^{bA}$ | 1657.98±2.09$^{cA}$ | 1657.35±1.01$^{bA}$ | 1656.51±1.95$^{aA}$ | 3.03 | 0.13 |
| | 50 | 1668.25±0.56$^{bA}$ | 1665.95±1.39$^{bA}$ | 1665.38±0.40$^{bA}$ | 1665.31±2.73$^{aA}$ | 1.26 | 0.38 |
| | 60 | 1675.74±0.80$^{aA}$ | 1673.70±1.06$^{aA}$ | 1672.46±2.10$^{aA}$ | 1672.11±3.43$^{aA}$ | 0.73 | 0.57 |
| | F-value | 7.98 | 23.41 | 54.04 | 65.44 | | |
| | P-value | 0.063 | 0.015 | 0.001 | 0.003 | | |
| **Flavonoids** | 40 | 3.95±0.17$^{aA}$ | 4.25±0.36$^{aA}$ | 4.28±0.41$^{aA}$ | 4.89±0.18$^{aA}$ | 2.97 | 0.14 |
| | 50 | 3.95±0.17$^{aA}$ | 3.98±0.61$^{aA}$ | 4.28±0.34$^{aA}$ | 4.37±0.00$^{aA}$ | 2.92 | 0.14 |
| | 60 | 3.74±0.00$^{aA}$ | 3.98±0.36$^{aA}$ | 3.98±0.41$^{aA}$ | 4.37±0.00$^{aA}$ | 2.96 | 0.13 |
| | F-value | 0.85 | 1.82 | 0.28 | 1.14 | | |
| | P-value | 0.51 | 0.30 | 0.77 | 0.38 | | |
| **Total Phenols** | 40 | 27.31±0.33$^{aA}$ | 26.97±0.61$^{aA}$ | 26.81±0.33$^{aA}$ | 26.66±0.63$^{aA}$ | 3.25 | 0.12 |
| | 50 | 25.85±0.42$^{aA}$ | 25.15±0.29$^{aA}$ | 24.89±0.78$^{aA}$ | 24.88±1.58$^{aA}$ | 0.29 | 0.83 |
| | 60 | 24.72±0.34$^{aA}$ | 24.67±1.37$^{aA}$ | 24.64±0.9M$^{aA}$ | 23.63±1.77$^{aA}$ | 1.74 | 0.27 |
| | F-value | 1.83 | 2.81 | 2.86 | 1.79 | | |
| | P-value | 0.30 | 0.21 | 0.20 | 0.25 | | |
| **Vitamin A** | 40 | 44.88±0.91$^{bA}$ | 44.27±1.29$^{bA}$ | 43.72±0.84$^{bA}$ | 42.36±1.73$^{bA}$ | 0.66 | 0.613 |
| | 50 | 49.83±0.89$^{aA}$ | 48.27±1.38$^{aA}$ | 46.59±2.06$^{aA}$ | 46.47±0.95$^{abA}$ | 1.67 | 0.287 |
| | 60 | 50.14±0.27$^{aA}$ | 49.83±0.89$^{Aa}$ | 49.27±0.37$^{aA}$ | 48.59±0.94$^{aA}$ | 0.63 | 0.62 |
| | F-value | 10.05 | 10.67 | 12.22 | 13.22 | | |
| | P-value | 0.046 | 0.046 | 0.031 | 0.006 | | |
| **Vitamin C** | 40 | 352.76±3.47$^{aA}$ | 350.24±3.9M$^{aA}$ | 350.02±7.64$^{aA}$ | 348.32±4.85$^{aA}$ | 0.11 | 0.95 |
| | 50 | 344.62±2.06$^{aA}$ | 341.88±2.04$^{aA}$ | 341.27±1.30$^{aA}$ | 339.79±0.95$^{bA}$ | 1.56 | 0.31 |
| | 60 | 336.60±1.05$^{aA}$ | 335.33±0.78$^{aA}$ | 335.22±0.93$^{aA}$ | 333.31±0.93$^{bA}$ | 1.74 | 0.27 |
| | F-value | 8.22 | 21.35 | 2.28 | 3.73 | | |
| | P-value | 0.061 | 0.017 | 0.089 | 0.25 | | |

The same lowercase letters indicate no significant difference across the temperatures, while the same uppercase letters indicate no significant difference among the pulp layer thickness according to the Tukey test at p = 0.05.

particular trend of an increase in L* values and a decrease in the E values across all the thicknesses and temperatures.

The decreased color change ΔE and increased L* could be attributed to color retention of the samples during the drying process due to the thin pulp layer and low drying temperatures (Vu et al., 2023). During the drying process of the tree tomato pulp, the decrease in temperature and increase in thickness may have caused the samples to become darker due to reactions of non-enzymatic browning, as evidenced by increased values of a* without significant variation in L* values (Nath Prerna and Pandey, 2022). Color is a significant quality attribute considered by processors and consumers of dried agricultural products, and they usually prefer color that matches the sources (İzli et al., 2022).

The sensory evaluation data of the dried tree tomato product (Fig. 5) showed that appearance and aroma were rated highest for the 6 mm samples dried at 60 °C while the taste and texture were more favorably rated for the 2 mm sample dried at 60 °C.

Table 6. Technological powder properties of 2, 4, 6, and 8 mm pulp layer thicknesses dried at 40, 50, and 60 °C.

| Properties | Drying temp. (°C) | Pulp layer thickness | | | | F-value | P-value |
|---|---|---|---|---|---|---|---|
| | | 2 mm | 4 mm | 6 mm | 8 mm | | |
| **Hygroscopicity** | 40 | 11.76±0.01$^{aA}$ | 11.75±0.06$^{aA}$ | 11.75±0.03$^{aA}$ | 11.75±0.03$^{aA}$ | 0.03 | 0.99 |
| | 50 | 11.32±0.04$^{bA}$ | 11.32±0.03$^{bA}$ | 11.32±0.02$^{Ba}$ | 11.32±0.00$^{bA}$ | 0.00 | 1.00 |
| | 60 | 10.56±0.01$^{cA}$ | 10.55±0.05$^{cA}$ | 10.55±0.05$^{cA}$ | 10.54±0.06$^{Ca}$ | 0.11 | 0.95 |
| | F-value | 154.85 | 230.35 | 1107.5 | 1212.1 | | |
| | P-value | 0.001 | 0.001 | <0.001 | <0.001 | | |
| **Rehydration Ratio** | 40 | 4.25±0.25$^{aA}$ | 4.50±0.00$^{aA}$ | 4.67±0.41$^{aA}$ | 4.75±0.75$^{aA}$ | 0.26 | 0.84 |
| | 50 | 4.25±0.25$^{aA}$ | 4.25±0.25$^{aA}$ | 4.50±0.20$^{aA}$ | 4.75±0.25$^{aA}$ | 0.66 | 0.61 |
| | 60 | 4.00±0.00$^{aA}$ | 4.25±0.25$^{aA}$ | 4.50±0.00$^{aA}$ | 4.67±0.20$^{aA}$ | 0.77 | 0.56 |
| | F-value | 0.50 | 0.30 | 3.50 | 0.07 | | |
| | P-value | 0.65 | 0.76 | 0.16 | 0.93 | | |
| **WSI_25** | 40 | 88.09±0.03$^{cA}$ | 88.23±0.04$^{cA}$ | 88.17±0.18$^{cA}$ | 88.05±0.03$^{cA}$ | 0.65 | 0.62 |
| | 50 | 95.35±0.12$^{bA}$ | 95.55±0.17$^{bA}$ | 95.43±0.11$^{bA}$ | 95.48±0.19$^{bA}$ | 0.31 | 0.82 |
| | 60 | 96.36±0.02$^{aA}$ | 96.55±0.13$^{aA}$ | 96.40±0.34$^{aA}$ | 96.24±0.07$^{aA}$ | 0.51 | 0.69 |
| | F-value | 4201.7 | 1296.0 | 375.29 | 1286.2 | | |
| | P-value | <0.001 | <0.001 | <0.001 | <0.001 | | |
| **WSI_50** | 40 | 91.15±0.10$^{bA}$ | 90.92±0.05$^{bA}$ | 91.01±0.08$^{bA}$ | 91.09±0.06$^{bA}$ | 1.77 | 0.27 |
| | 50 | 98.67±0.09$^{aA}$ | 98.44±0.01$^{aA}$ | 98.58±0.14$^{aA}$ | 98.57±0.40$^{aA}$ | 0.16 | 0.92 |
| | 60 | 99.12±0.06$^{aA}$ | 98.95±0.03$^{aA}$ | 99.09±0.07$^{aA}$ | 99.04±0.08$^{aA}$ | 1.04 | 0.45 |
| | F-value | 2649.7 | 21094 | 1979.4 | 604.89 | | |
| | P-value | <0.001 | <0.001 | <0.001 | <0.001 | | |
| **WSI_80** | 40 | 90.70±0.03$^{cA}$ | 90.78±0.01$^{cA}$ | 90.73±0.08$^{cA}$ | 90.73±0.15$^{cA}$ | 0.04 | 0.99 |
| | 50 | 97.79±0.18$^{bA}$ | 97.91±0.33$^{bA}$ | 97.96±0.13$^{bA}$ | 97.97±0.02$^{bA}$ | 0.25 | 0.86 |
| | 60 | 99.32±0.06$^{aA}$ | 99.27±0.28$^{aA}$ | 99.80±0.02$^{aA}$ | 99.19±0.18$^{aA}$ | 1.56 | 0.31 |
| | F-value | 1805.8 | 327.88 | 2909.8 | 661.28 | | |
| | P-value | <0.001 | <0.001 | <0.001 | <0.001 | | |

The same lowercase letters indicate no significant difference across the temperatures, while the same uppercase letters indicate no significant difference among the pulp layer thickness according to the Tukey test at p = 0.05.

The sensory attributes of the tree tomato pulp of 2 mm thickness dried at 60 °C gave the best quality results as compared to the other samples. This could be as a result of fast and even drying of the pulp, resulting in superior sensory quality attributes, which are important quality indicators in food industries. The hedonic scale rating of the tree tomato powder showed it was within the acceptable consumer range (Lawless & Heymann, 2010).

The functional properties (antioxidant activity, flavonoids, total phenols, vitamin A and C) are shown in Table 5. There was a significant ($p < 0.05$) effect on the antioxidant activity, and vitamins A and C of the dried tree tomato pulp product. There was an increase in the antioxidant activity across the drying temperatures and different pulp layer thicknesses. There were no significant ($p > 0.05$) differences in the flavonoids and total phenols, as the samples retained the properties at the different drying temperatures across all the pulp layer thicknesses. Vitamin A and C results show that there was a significant ($p < 0.05$) difference across the drying temperatures, but no effect caused by the pulp layer thicknesses.

The functional properties (antioxidant activity, flavonoids, total phenols, and vitamins A and C) are sensitive to internal and external factors that could affect their retention during the drying process. Samples dried at a temperature of 60 °C recorded higher total phenols, and this may be because of the non-enzymatic interconversion between phenolic molecules, which form precursors of phenolic compounds. Also, the reduced drying time at 60 °C as opposed to 40°C might have stopped the phenolic compound from degrading thermally and oxidatively (Rajoriya et al., 2021). Irrespective of the thickness of the tomato pulp layer during drying, the samples retained the highest total phenols content at 60 °C. Similar retention was recorded during drying of pumpkin powder and banana puree at different temperatures (İzli et al., 2022 ; Rajoriya et al., 2021). The highest antioxidant activity was recorded across all sample thicknesses dried at 60 °C as compared to those dried at 40 °C. Drying the samples at a higher temperature reduced the drying time, and this could have contributed to the higher levels of antioxidant activity retention. There was a direct relationship between the antioxidant activity and total phenol retention in the samples. The fast rate of moisture withdrawal from the samples could have helped in the release of phenolic compounds from the tree tomato product cells and also prevented too much exposure of the antioxidant compounds, which could have led to their deterioration (Akther et al., 2023).

Vitamin C is a biological antioxidant mainly found in vegetables and fruits. It is an indicator of quality for processed food, as it is sensitive to processing variables like drying time, moisture content, temperature, light, oxygen, pH, and catalyzing agents. At temperatures of 40 °C, lower values of vitamin C were recorded than at 60 °C, and this could be attributed to the prolonged period of drying, which led to exposure of the samples to the above factors, which could have led to oxidation and loss (İzli et al., 2022). During the drying process, vitamin C is lost due to increased temperature and prolonged exposure, leading to oxidation or utilization of the ascorbic acid to shield polyphenols from oxidation (Kamiloglu et al., 2016). Recent studies have shown that vitamin C usually decreases during the drying of fruits like oven-dried apples (Kamiloglu et al., 2016) and mangos (Vu et al., 2023). Vitamin A activity and value are usually contained in fruits and vegetables as beta-carotene and have high antioxidant potential, and scavenge peroxyl radicals. However, it is prone to degradation during processing (Ordóñez-Santos & Martínez-Girón, 2020). Higher values of vitamin A were recorded at temperatures of 60 °C as compared to 40 °C, and this could be due to the shorter period of drying and less exposure time to oxidation. Work done on drying apricots using a hot-air oven

witnessed a similar trend to the tree tomato product (Kamiloglu et al., 2016).

The technological properties (hygroscopicity and water solubility index) showed significant differences across the drying temperatures and thicknesses. In contrast, the rehydration ratio showed no significant difference across the pulp layer thickness and drying temperatures (Table 6). The water solubility indexes of the tree tomato powder were determined at 25, 50, and 80 °C and were highest at 80 °C.

The water solubility index (WSI) is used to determine the technological aspect of reconstituting the tree tomato powder. The increase in temperature impacted the powder solubility, with the highest recorded at while the lowest was at. That shows the solubility index increased with the increase in temperature (Senanayake et al., 2013). During the drying process, the temperature affects the sugar component of the fruit product, causing a change of the molecular structure from the crystalline sugar structure state to the amorphous state, affecting its water solubility. Powdered food products, including the tree tomato powder product under study, should have the unique characteristic of promptly dissolving in water. The powder particles should immediately wet, then sink and disperse in the water without forming lumps or floating (İzli et al., 2022).

The rehydration ratio is a critical quality metric for dried foods that is influenced by the product's composition and processing conditions, and the capacity to reconstitute depends on the internal structures of the dried food material and the degree of drying-induced damage to the water-holding components, such as starch (Kahraman et al., 2021). A high ratio is strongly correlated with higher water reabsorption, which is an indicator that the product's structure and physical changes are minimally affected during the drying process (Aravindakshan et al., 2021). The results did not show any significant effect of the drying temperatures and pulp layer thickness on the rehydration property, which is a significant quality attribute for fruit powder products, usually influenced by drying conditions and the product composition (Ong et al., 2020).

The hygroscopicity of the tree tomato powder is its propensity to absorb moisture from a higher relative humidity environment and to balance out with the surroundings (Hssaini et al., 2020).

The hygroscopic nature is due to the polar ends of the tree tomato powder, which interact strongly with water molecules, increasing their hygroscopicity, and this potentially influences the powder quality. The hygroscopicity decreased with an increase in temperature, and this could be attributed to the effect of the moisture content of the powder, whereby when dried at higher temperatures, it lost more water and was more hygroscopic (Hadree et al., 2023). This was in agreement with (Hssaini et al., 2020), who found that low moisture content of powder product increases its hygroscopicity.

## 4. Conclusion

The drying rate of tree tomato pulp varied with an increase in temperature and pulp layer thickness. The Modified Page model emerged as the most appropriate for simulating the drying process, demonstrating a superior fit to the experimental data. The constant values of n across all thicknesses suggest that the shape of the drying curve, representing the drying mechanism, was more influenced by temperature than thickness. This consistency implies a similar moisture removal mechanism across different thicknesses when exposed to the same drying conditions, albeit at different rates. The physicochemical, technological, and functional properties varied with an increase in temperature and the pulp layer thickness. There was a high retention of the bioactive compounds, physicochemical, and technological features of the dry product, with potential for use in food applications.

The findings can be used in process engineering to develop unique shelf-stable products such as nutraceuticals, tablets, and/or natural food ingredients for dairy and baking applications. More research is required to comprehend how the characteristics of the tree tomato fruit powder product after reconstitution alter extended periods of storage, the nutritive value, and consumer perception.

## Acknowledgements and foundation

The authors thank the FoodLAND project for funding the research.

FoodLAND project through funding from the European Union's Horizon 2020 research and innovation program under grant agreement (GA No 862802).

## Conflict of interest

The authors declare that there is no conflict of interest.

## Data Availability

The data supporting the findings of this study are available from the corresponding author, [Maitha, I.M.], upon request.

## References

Akther, S., Sultana, J., Badsha, R., Rahman, M., Buddha, G., & Alim, A. (2023). Drying methods effect on bioactive compounds, phenolic profile, and antioxidant capacity of mango powder. *Journal of King Saud University - Science*, *35*(1), 102370. https://doi.org/10.1016/j.jksus.2022.102370

AOAC. (2010). Official Methods of Analysis: 18th Edition,2005. In *TrAC Trends in Analytical Chemistry* (Vol. 9, Issue 4). https://doi.org/10.1016/0165-9936(90)87098-7

Aravindakshan, S., Nguyen, T. H. A., Kyomugasho, C., Buvé, C., Dewettinck, K., Van Loey, A., & Hendrickx, M. E. (2021). The impact of drying and rehydration on the structural properties and quality attributes of pre-cooked dried beans. *Foods*, *10*(7). https://doi.org/10.3390/foods10071665

Azeez, L., Adebisi, S. A., Oyedeji, A. O., Adetoro, R. O., & Tijani, K. O. (2019). Bioactive compounds' contents, drying kinetics and mathematical modelling of tomato slices influenced by drying temperatures and time. In *Journal of the Saudi Society of Agricultural Sciences* (Vol. 18, Issue 2, pp. 120–126). King Saud University & Saudi Society of Agricultural Sciences. https://doi.org/10.1016/j.jssas.2017.03.002

Bhagya Raj, G. V. S., & Dash, K. K. (2022). Comprehensive study on applications of artificial neural network in food process modeling. In *Critical Reviews in Food Science and Nutrition* (Vol. 62, Issue 10, pp. 2756–2783). Taylor and Francis Ltd. https://doi.org/10.1080/10408398.2020.1858398

Bhattacharjee, S., Mohanty, P., Sahu, J. K., & Sahu, J. N. (2024). A critical review on drying of food materials: Recent progress and key challenges. *International Communications in Heat and Mass Transfer*, *158*, 107863.

https://doi.org/10.1016/J.ICHEATMASSTRANSFER.2024.107863

Chibuzo, N. S., Osinachi, U. F., James, M. T., Chigozie, O. F., Dereje, B., & Irene, C. E. (2021). Technological advancements in the drying of fruits and vegetables: A review. *African Journal of Food Science*, *15*(12), 367–379. https://doi.org/10.5897/AJFS2021.2113

Dhande, A., Agarwal, M., & Agarwal, G. Das. (2024). Drying kinetics (mathematical modeling) and quality evaluation of herbal leaves (Adulsa and Durva) dried in small-scale greenhouse solar dryer (GHSD): Experimental investigation and comparative analysis. *Journal of Food Process Engineering*, *47*(8). https://doi.org/10.1111/jfpe.14704

Djebli, A., Hanini, S., Badaoui, O., Haddad, B., & Benhamou, A. (2020). Modeling and comparative analysis of solar drying behavior of potatoes. *Renewable Energy*, *145*, 1494–1506. https://doi.org/10.1016/j.renene.2019.07.083

Doymaz, I. (2014). Drying kinetics and rehydration characteristics of convective hot-air dried white button mushroom slices. Journal of Chemistry, 2014. https://doi.org/10.1155/2014/453175ng

Dufera, L. T., Hofacker, W., Esper, A., & Hensel, O. (2023). Effect of packaging materials on lycopene vitamin C and water activity of dried tomato (Lycopersicon esculentum Mill.) powder during storage. *Food Science and Nutrition*, *May*, 1–8. https://doi.org/10.1002/fsn3.3562

García, J. M., Prieto, L. J., Guevara, A., Malagon, D., & Osorio, C. (2016). Chemical studies of yellow tamarillo (Solanum betaceum Cav.) fruit flavor by using a molecular sensory approach. *Molecules*, *21*(12), 1–11. https://doi.org/10.3390/molecules21121729

Hadree, J., Shahidi, F., Mohebbi, M., & Abbaspour, M. (2023). Evaluation of Effects of Spray Drying Conditions on Physicochemical Properties of Pomegranate Juice Powder Enriched with Pomegranate Peel Phenolic Compounds: Modeling and Optimization by RSM. In *Foods* (Vol. 12, Issue 10). https://doi.org/10.3390/foods12102066

Hssaini, L., Ouaabou, R., Charafi, J., Idlimam, A., Lamharrar, A., Razouk, R., & Hanine, H. (2020). Hygroscopic proprieties of fig (Ficus carica L.): Mathematical modelling of moisture sorption isotherms and isosteric heat kinetics. *South African Journal of Botany*, *000*. https://doi.org/10.1016/j.sajb.2020.11.026

Inyang, U. E., Oboh, I. O., & Etuk, B. R. (2018). Kinetic Models for Drying Techniques—Food Materials. *Advances in Chemical Engineering and Science*, *08*(02), 27–48. https://doi.org/10.4236/aces.2018.82003

İzli, G., Yildiz, G., & Berk, S. E. (2022). Quality retention in pumpkin powder dried by combined microwave-convective drying. *Journal of Food Science and Technology*, *59*(4), 1558–1569. https://doi.org/10.1007/s13197-021-05167-5

Jideani, A. I. O., & Anyasi, T. A., (Eds.). (2020). *Banana Nutrition - Function and Processing Kinetics. Intech Open. Https://Doi.Org/10.5772/Intechopen.76736*, *11*(tourism), 13.

Kahraman, O., Malvandi, A., Vargas, L., & Feng, H. (2021). Drying characteristics and quality attributes of apple slices dried by a non-thermal ultrasonic contact drying method. *Ultrasonics Sonochemistry*, *73*, 105510. https://doi.org/10.1016/J.ULTSONCH.2021.105510

Kamiloglu, S., Toydemir, G., Boyacioglu, D., Beekwilder, J., Hall, R. D., & Capanoglu, E. (2016). A Review on the Effect of Drying on Antioxidant Potential of Fruits and Vegetables. *Critical Reviews in Food Science and Nutrition*, *56*, S110–S129. https://doi.org/10.1080/10408398.2015.1045969

Lawless, H. T., & Heymann, H. (2010). Sensory evaluation of food: principles of good practice. In *Sensory Evaluation of Food*. https://doi.org/10.1007/978-1-4419-6488-5

Liu, Y., Zhang, Z., & Hu, L. (2022). High efficient freeze-drying technology in food industry. In *Critical Reviews in Food Science and Nutrition* (Vol. 62, Issue 12, pp. 3370–3388). Taylor and Francis Ltd. https://doi.org/10.1080/10408398.2020.1865261

Loha, C., Das, R., & Choudhury, B. (2012). Evaluation of Air Drying Characteristics of Sliced Ginger (Zingiber officinale) in a Forced Convective Cabinet Dryer and Thermal Conductivity Measurement. *Journal of Food Processing & Technology*, *03*(06). https://doi.org/10.4172/2157-7110.1000160

Madani, N., & Sharifi, A. (2020). Beverage powder based on Shahani grape pomace extract: Physicochemical properties of foam-mat freeze-dried and spray-dried powders. https://doi.org/10.22059/JFABE.2024.375744.1172

Mahanti, N. K., Chakraborty, S. K., Sudhakar, A., Verma, D. K., Shankar, S., Thakur, M., Singh, S., Tripathy, S., Gupta, A. K., & Srivastav, P. P. (2021). Refractance WindowTM-Drying vs. other drying methods and effect of different process parameters on quality of foods: A comprehensive review of trends and technological developments. *Future Foods*, *3*(March), 100024. https://doi.org/10.1016/j.fufo.2021.100024

Maitha, I. M., Okoth, M. W., Njue, L. G., & Mbuge, D. O. (2025). Characterization of the attributes impacting industrial adoption of tree tomato fruit varieties in Kenya. *Cogent Food and Agriculture*, *11*(1). https://doi.org/10.1080/23311932.2025.2464226

Mewa, E. A., Okoth, M. W., Kunyanga, C. N., & Rugiri, M. N. (2019). Experimental evaluation of beef drying kinetics in a solar tunnel dryer. *Renewable Energy*, *139*, 235–241. https://doi.org/10.1016/j.renene.2019.02.067

Muzaffar, K., & Kumar, P. (2016). Comparative efficiency of maltodextrin and protein in the production of spray-dried tamarind pulp powder. *Drying Technology*, *34*(7), 802–809. https://doi.org/10.1080/07373937.2015.1080724

Nadian, M. H., Abbaspour-Fard, M. H., Martynenko, A., & Golzarian, M. R. (2017). An intelligent integrated control of hybrid hot air-infrared dryer based on fuzzy logic and computer vision system. *Computers and Electronics in Agriculture*, *137*, 138–149. https://doi.org/10.1016/j.compag.2017.04.001

Nath Prerna, Pandey, N. and S. M. and S. K. and K. S. and K. P. and S. S. and C. O. P. (2022). Browning Reactions in Foods. In O. P. Chauhan (Ed.), *Advances in Food Chemistry: Food Components, Processing and Preservation* (pp. 117–159). Springer Nature Singapore. https://doi.org/10.1007/978-981-19-4796-4_4

Nedamani, A. R., & Hashemi, S. J. (2020). *RSM-CFD modeling for optimizing the apricot water evaporation*. https://doi.org/10.22059/jfabe.2021.320809.1088

Nwakuba, N., Ezeanya, N., Horsfall, I. T., Okafor, V., Ononogbo, C., Ndukwu, M., Simo-Tagne, M., & Asoegwu, S. (2025). Heat and moisture transport in okra cylinders with shrinkage effects under solar drying: a multiphysics-based simulation approach (pp 117–159) *Sustainable Food Technology*. https://doi.org/10.1039/d4fb00343h

Ong, X. Y., Taylor, S. E., & Ramaioli, M. (2020). Rehydration of food powders: Interplay between physical properties and process conditions. *Powder Technology*, *371*, 142–153. https://doi.org/10.1016/J.POWTEC.2020.05.066

Ordóñez-Santos, L. E., & Martínez-Girón, J. (2020). Thermal degradation kinetics of carotenoids, vitamin C and provitamin A in tree tomato juice. *International Journal of Food Science and Technology*, *55*(1), 201–210. https://doi.org/10.1111/ijfs.14263

Raghavi, L. M., Moses, J. A., & Anandharamakrishnan, C. (2018). Refractance window drying of foods: A review. *Journal of Food Engineering*, *222*, 267–275. https://doi.org/10.1016/j.jfoodeng.2017.11.032

Rajoriya, D., Bhavya, M. L., & Hebbar, H. U. (2021). Impact of process parameters on drying behaviour, mass transfer and quality profile of refractance window dried banana puree. *Lwt*, *145*(November 2020), 111330. https://doi.org/10.1016/j.lwt.2021.111330

Schmidt, S. J. (2020). Water Mobility in Foods. *Water Activity in Foods*, *1957*, 61–122. https://doi.org/10.1002/9781118765982.ch5

Senanayake, S., Gunaratne, A., Ranaweera, K., & Bamunuarachchi, A. (2013). Effect of Heat Moisture Treatment Conditions on Swelling Power and Water-Soluble Index of Different Cultivars of Sweet Potato (Ipomea batatas (L). Lam) Starch. *ISRN Agronomy*, *2013*, 1–4. https://doi.org/10.1155/2013/502457

Sharifi, A., Niakousari, M., & Rigi, S. (2020). *Experimental study and mathematical modeling of thin layer drying of rhubarb (Rheum ribes L.)*. https://doi.org/10.22059/jfabe.2020.75287

Snoussi, A., Essaidi, I., Ben, H., Koubaier, H., Zrelli, H., Alsafari, I., Živoslav, T., Mihailovic, J., Khan, M., & Omri, A. El. (2021). Drying methodology effect on the phenolic content, antioxidant activity of Myrtus communis L. leaves ethanol extracts and soybean oil oxidative stability. *BMC Chemistry*, 1–11. https://doi.org/10.1186/s13065-021-00753-2

Tapia, M. S., Alzamora, S. M., & Chirife, J. (2020). Effects of water activity (aw) on microbial stability as a hurdle in food preservation. *Water Activity in Foods: Fundamentals and Applications*, 323–355. https://doi.org/10.1002/9781118765982.ch14

Van 'T Hag, L., Danthe, J., Handschin, S., Mutuli, G. P., Mbuge, D., & Mezzenga, R. (2020). Drying of African leafy vegetables for their effective preservation: The difference in moisture sorption isotherms explained by their microstructure. *Food and Function*, *11*(1), 955–964. https://doi.org/10.1039/c9fo01175g

Verma, T., Wei, X., Lau, S. K., Bianchini, A., Eskridge, K. M., & Subbiah, J. (2018). Evaluation of Enterococcus faecium NRRL B-2354 as a Surrogate for Salmonella During Extrusion of Low-Moisture Food. *Journal of Food Science*, *83*(4), 1063–1072. https://doi.org/10.1111/1750-3841.14110

Vu, N. D., Nguyen, V. M., & Tran, T. T. (2023). Effects of pH, Total Soluble Solids, and Pectin Concentration on Color, Texture, Vitamin C, and Sensory Quality of Mango Fruit Bar. *International Journal of Food Science*, *2023*. https://doi.org/10.1155/2023/6618300

Xu, J., Wang, P., Bai, Z., Cheng, H., Wang, R., Qu, L., & Li, T. (2024). Sustainable moisture energy. *Nature Reviews Materials*, *9*(10), 722–737. https://doi.org/10.1038/s41578-023-00643-0